Computational Analysis of Impulse Generation Mechanisms in Intense Laser-Solid Interaction

Takeharu Sakai*
Nagoya University, Nagoya, 464-8603, Japan
Kohei Anju†, Kensuke Sawada‡,
Tohoku University, Sendai, 980-8579, Japan
Koichi Mori§, and Akihiro Sasoh¶
Nagoya University, Nagoya, 464-8603, Japan

A computational technique is developed to study the impulse generation mechanisms with the laser ablation of a solid material. One-dimensional heat conduction equation of a solid material is solved to calculate vaporizing, melting, and heat-conducting process of the material irradiated by a laser beam. Vaporized plume expansion process into a background gaseous environment is calculated by solving one-dimensional Euler equations. The plume of the ablated material is assumed to be a local thermal equilibrium plasma, and the emission and laser beam absorption of the plasma are accounted for in the calculation of the plume expansion process. The flow calculation is coupled with the heat conduction calculation. The technique is applied to compute the time variation of the impulse data for the ablation of an aluminum target using Nd:YAG laser. The computed results are compared with the measurement conducted using the Velocity Interferometer System for Any Reflector(VISAR).

Nomenclature

C_{pl} = specific heat of liquid aluminum , 901 J/(kg K)
C_{ps} = specific heat of solid aluminum , 2229 J/(kg K)
c = velocity of light, 2.998×10^8 m/s
e = elementary electrical charge, 1.602×10^{-19} C
E_L = incident laser specific intensity, W/m^2
h = Planck constant, 6.626×10^{-34} J·s
I_{ion} = First ionization energy, 48,318 cm^{-1}
k = Boltzmann constant, 1.381×10^{-23} J/k
m = mass, kg
n = number density, m^{-3}
p = pressure, Pa
Q = partition function
R_f = reflectivity
R_u = universal gas constant, 8.314 J/(mol K)
x = coordinate in flowfield, m
T = temperature, K
T_m = melting temperature, 933.5 K
T_{bp} = normal boiling temperature, 2740 K

*Associate Professor, Department of Aerospace Engineering
†Graduate Student, Department of Aeronautics and Space Engineering
‡Professor, Department of Aeronautics and Space Engineering
§Associate Professor, Department of Aerospace Engineering
¶Professor, Department of Aerospace Engineering

t = time, sec
u = velocity, m/s
z = coordinate within solid, m
ΔH_m = latent heat of fusion, 10.3 kJ/mol
ΔH_v = latent heat of fusion at normal boiling point, 288.3 kJ/mol
ϵ = emission energy density, W/m^3
$\tilde{\epsilon}$ = internal energy, J/m^3
κ = thermal conductivity, W/(m K)
κ_l = thermal conductivity of liquid alminum, 100 W/(m K)
κ_s = thermal conductivity of solid alminum, 225 W/(m K)
λ = laser wavelength, m
ρ = density, kg/m^3
ρ_l = density of liquid alminum, 2700 kg/m^3
ρ_s = density of solid alminum, 2700 kg/m^3
η = degree of ionization

Subscripts

a = atom
B = Bremsstrahlung
b = background ambient gas
bp = boiling point
e = electron
IB = Inverse Bremsstrahlung
i = ion
int = liquid-vapor interface
l = liquid
m = melt
s = solid
sf = surface of a solid
t = target
v = vapor

I. Introduction

The impulse generated by the interaction of pulsed laser with a solid target is expected to be used for a number of space technology applications such as propulsion in space and a removal method of space debris, and a launch system to space.[1] A key issue to develop such space technologies by using laser power is to understand the impulse generation mechanisms during the ablation of the solid by the pulsed laser heating. Because laser ablation phenomenon is affected by a number of physical parameters such as target thermophysical characteristics, laser wavelength, laser intensity and pulse duration, and an ambient gas pressure, and so on, we must examine the impact of these parameters on the generation of the impulse and must know how efficiently the impulse can be produced by changing these physical parameters.

Recently, the time variation of the surface pressure of a solid target irradiated pulsed-laser beam is measured using a velocity interferometer called VISAR (Velocity Interferometer System for Any Reflector).[1,2] Figure 1 shows the schematic diagram of the laser ablation measurement using VISAR system. In VISAR, the velocity of the back-surface target in motion is measured based on a velocity interferometer using an optical detecting system. The impulse is evaluated by integrating the pressure on the local surface of the target. Further details are given in the papers,[1,2] and are omitted here. Measurements are carried out using Nd:YAG laser with the laser wavelength of 1064 nm or CO_2 laser with 10.6 μm. Aluminum and polyacetal are used as the target material. The ambient environment is filled with air. The measurement are made under the different ambient pressure ranging 10^{-2} to 10^5 Pa.

Laser ablation phenomenon is not well understood yet. Extensive efforts have been made to numerically simulate laser ablation phenomenon for various purposes.[3] The real-time impulse data measured by Sasoh et al. offer an opportunity to validate the current computational capabilities. It is the purpose of the present work to develop a computational method to calculate laser ablation phenomenon. The method will be used

to analyze the impulse generation mechanism during laser ablation.

The present paper is a progress report. A preliminary result is presented for the case of laser ablation of alminum target using Nd:YAG laser. Calculation is made for the case of the ambient pressure of 10^{-2} Pa. Calculated impulse data is compared with the measured real-time impulse data for the validation of the numerical method developed in the present work.

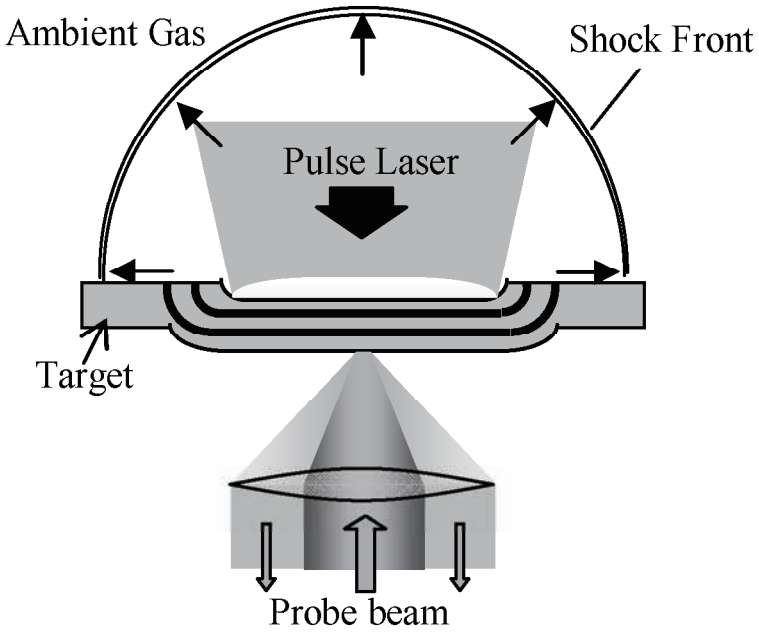

Figure 1. Schematic diagram of laser-ablative impulse measurement using VISAR

II. Numerical and Physical Modeling

In order to simulate laser ablation phenomenon, the flowfield that vaporized material expands and the heat conduction within aluminum solid target irradiated laser beam are calculated simultaneously. Various analytical models for the simulation of laser ablation are reviewed by Bogaerts et al.[3] Although a detailed explanation for the models is given therein, the present method is briefly explained next.

A. Flowfield

The expansion process of the metallic vapor produced by the ablation of solid aluminum is calculated using a computational fluid dynamics technique. The one-dimensional inviscid flow is assumed to be perfect gas. Mass, momentum, and energy conservation equations are solved using a finite volume method. The conservation equations can be written as

$$\frac{\partial \mathbf{Q}}{\partial t} + \frac{\partial \mathbf{F}}{\partial x} = \mathbf{S}$$

$$\mathbf{Q} = \begin{pmatrix} \rho_v \\ \rho_b \\ \rho u \\ e \end{pmatrix} \mathbf{F} = \begin{pmatrix} \rho_v u \\ \rho_b u \\ \rho u^2 + p \\ (e+p)u \end{pmatrix} \mathbf{S} = \begin{pmatrix} 0 \\ 0 \\ 0 \\ \kappa^{IB} E_L - \epsilon_B \end{pmatrix}$$

where $\rho = \rho_v + \rho_b$. ρ_b denotes the background ambient gas, and air is used as was in the experiment.[1,2] The air is represented by a perfect gas with the specific heat of 1.4. The gas pressure is given by the equation of state for perfect gas

$$p - (1+\eta) n_v kT + n_b kT.$$

Unsteady solutions are obtained by numerically integrating the equations using an Euler explicit method. Computed flow properties are second order accurate in space using the MUSCL approach. the primitive variables (ρ, u, p) are interpolated in the MUSCL approach. The numerical flux function is evaluated using the AUSM-DV scheme.[4] For the boundary condition at the vaporizing surface, the numerical flux function is calculated similarly by specifying the vapor properties such as density, velocity and pressure in a ghost cell. These properties will be explained in a later subsection. The source term $\mathbf{S}$ represents the loss and gain of the internal energy by radiation emission and absorption. The first term in the radiative source term stands for the absorption of laser intensity, and the second one represents the emission from the high temperature vaporized gas. These terms will be explained more details next.

Because the temperature of the metallic vapor plasma becomes the order of 10^4 K, the vapor is ionized and strong emission occurs. In addition, incident laser energy is absorbed by the ionized plasma, resulting that the laser beam incident onto the material target would be weaken. The thermal radiation process is represented by the continuum radiation which consists mainly of free-free transition. In the present study, the absorption and emission characteristics in the free-free transition is calculated assuming that local thermodynamic equilibrium is established.[3]

The total amount of energy emitted by the free-free transition can be written as follows[5]

$$c_B = \begin{pmatrix} 2\pi kT \\ 3m_e \end{pmatrix}^{\frac{1}{2}} \begin{matrix} 32\pi e^6 \\ 3hm_e c^3 \end{matrix} n_e n_i$$

The absorption coefficient is given by the sum of the contributions between electron and atom, and between electron and ion, as follows:[6]

$$\begin{aligned} \kappa^{IB} &= \kappa^{IB}_{e-i} + \kappa^{IB}_{e-i} \\ \kappa^{IB}_{e-a} &= \left\{ 1 - \exp\left(-\frac{hc}{\lambda kT} \right) \right\} Q n_e n_i \\ \kappa^{IB}_{e-i} &= \left\{ 1 - \exp\left(-\frac{hc}{\lambda kT} \right) \right\} \frac{4e^6 \lambda^3}{3hcm_e} \left(\frac{2\pi}{3m_e kT} \right)^{\frac{1}{2}} \end{aligned}$$

The ionized state of the plasma vapor in the local thermodynamic equilibrium state is calculated by using the Saha equation

$$\frac{\eta^2}{1-\eta} = 2\frac{Q_i}{Q_a}\frac{1}{n_v}\left(\frac{2\pi m_e kT}{h^2} \right)^{\frac{3}{2}} \exp\left(-\frac{1.439 I_{ion}}{T} \right) \tag{1}$$

At present, we consider only a singly ionization reaction in the present study. The internal energy is given by

$$\bar{\epsilon} = \left\{ \frac{3}{2}(1+\eta)kT + b_1 I_{ion}\eta \right\} n_v \tag{2}$$

where the symbol b_1 stands for an energy conversion factor from cm^{-1} to Joule. In order to calculate the ionization fraction η, and temperature T, Eqs.(1) and (2) are solved by an iterative procedure.

The laser beam intensity incident on the target, E_L, could be attenuated by the absorption of the plasma. This process is calculated by using Beer-Lambert law in the present study.

B. Heat conduction in solid target and vaporization

In order to calculate the pulsed laser heating of aluminum solid including melting and evaporation, one-dimensional heat diffusion equation is solved. Because the absorption length of the laser radiation is of the order of 10^{-7} m, the penetration of the laser radiation into the target is neglected and the laser radiation is assumed to be completely absorbed at the surface of the target.[7] The heat diffusion equation can be written as

$$\frac{\partial H_t}{\partial t} - v_{int}\frac{\partial H_t}{\partial z} = \frac{\partial}{\partial z}\left(\kappa_t \frac{\partial T_t}{\partial z} \right)$$

where z is the moving coordinate attached with the liquid-vapor interface. By assuming that the enthalpy H_t is a function of temperature, the temperature within the target is evaluated as follows:

$$T = \begin{cases} {H_t}/{\rho_s C_{p_s}} & H_t \leqslant \rho C_{p_s} T \\ T_{melt} & \rho_s C_{p_s} T < H_t \leqslant \rho_s C_{p_s} T_{melt} + Q_{melt} \\ T_{melt} + {(H_t - \rho_s C_{p_s} T_{melt} - \Delta H_m)}/{\rho_l C_{p_l}} & H_t > \rho_s C_{p_s} T_{melt} + \Delta H_m \end{cases}$$

The equation is discretized using the finite volume method, and solutions are obtained by integrating the discretized using an explicit method. The adiabatic condition is specified at $z = \infty$. The boundary condition at $z = 0$ is given by

$$\left(\kappa_t \frac{\partial T_t}{\partial z}\right)_{z=0} = \rho_l \Delta H_v v_{int} - (1 - R_f) E_L$$

Although the surface reflectivity R_f is believed to be reduced as the surface temperature increases, the surface reflectivity is taken to be a constant value of 0.83 in the present study. This value is determined iteratively to replicate the experimental impulse value for the case of the background ambient pressure of $10{-}2$ Pa.

The velocity of the liquid-vapor interface is determined from the flux of atoms leaving from the interface as follows:

$$v_{int} = \frac{p_v}{\rho_l \left(2\pi k T/m\right)} \tag{3}$$

where the sticking coefficient is taken to be unity in Eq. (3). The vapor pressure p_v can be calculated by using the Clasius-Clapeyron equation with the surface temperature T:

$$p_v = p_0 \exp\left\{\frac{\Delta H_v (T_{sf} - T_{bp})}{R_g T_{sf} T_{bp}}\right\} \tag{4}$$

where p_0 is 1 atm.

The vapor density, velocity, and pressure values at the evaporating surface are necessary in order to calculate the expansion of the ablated material. These values are used as the boundary condition in the CFD calculations explained earlier. The vapor pressure is given by Eq.4. The vapor density is calculated by using the vapor pressure

$$\rho_v = \frac{p_v m}{k T_{sf}}$$

The velocity of vapor leaving from the surface is given by assuming that the particles have a Maxwellian distribution

$$v_v = \left(\frac{2kT_{sf}}{\pi m}\right)^{\frac{1}{2}}.$$

Initial conditions are as follows: the ambient pressure and temperature in flowfield are taken to be $10^{\ -2}$ Pa and 300 K, respectively. The temperature within the target is taken to be 300 K. The 201 grid points (200 computational cells) are used for the flowfield. The non-uniform spacing grid is used and the minimum spacing adjacent to the target boundary is taken to be 10 nm. For the heat conduction equation, the 1001 grid points with the uniform spacing of 20 nm. The global time step is determined by comparing the minimum time step between for the heat conduction calculation and for the flowfield calculation. The value of the time step size is typically of the order of 10^{-14} s in the present study. Thermophysical parameters of aluminum are summarized in Nomenclature.

III. Results and Discussion

The present numerical method is applied to calculate the pulse laser ablation experiment using aluminum target for the case of the background ambient gas pressure of 10^{-2} Pa. Figure 2 shows the time variation of the incident laser intensity. Two laser intensity profiles are given in the figure for the cases with and

without the laser beam attenuation by the vapor plasma. The profile with attenuation stands for the laser intensity reaching at the target surface after passing through the plume of the vaporized material. Note that the intensity profile without attenuation is taken from the experimental laser output measured using a photon detector and is here given for the purpose of comparison. The duration time of the laser pulse is approximately 18 ns. From the intensity profile with attenuation, one can see that the intensity is abruptly reduced at the time of about 10 ns. This is due to the absorption of the original laser beam by the expanding plasma produced by the ablation of the target. After this reduction, the laser intensity increases again. Because the vapor plasma emits strong radiation, the internal energy of the vapor plasma is reduced and the temperature is decreased. As a result, the absorption by the vapor plasma is weaken.

In Fig. 3, the calculated surface temperature is plotted against time. The target begins to melt at about 1 ns after the pulsed laser heating. The evaporation starts at about 5 ns, and the total evaporated depth is approximately 50 nm, though the results are not shown here. The surface temperature reaches the maximum value of 5,650 K at about 10 ns. This time is correspond to the moment that the laser beam is attenuated as was explained in Fig. 2. After reaching the maximum temperature, the surface temperature gradually decreases. It should be noted that a small increase in the temperature profile after the maximum point is correspond to the second increase in the laser intensity profile seen in Fig. 2, as was described earlier.

Figures 4(a)-4(d) show the spatial distribution of the calculated temperature, pressure, velocity, and density of the expanding vapor plasma, respectively. In the figure, the results are presented for three different times, 5 ns, 10 ns, and 20 ns, respectively. It is seen from Fig. 4(a) that the vapor temperature in the thinner region near the wall increases rapidly up to 10 ns. This increase is due partly to the pulsed laser heating mainly to the absorption of the pulsed laser light by the vapor plasma. The temperature becomes the order of 10,000 to 60,000 K. The vapor temperature is decreased after 10 ns as the plume expands. The plateau of the temperature profile at 20 ns is seen from x=0.00025 to 0.00035 m. This relatively low temperature region is the result of the internal energy loss by the emission of radiation. From Fig. 4(b), the vapor pressure gradually drops apart from the target surface, and the pressure profile has its highest value near the target surface. One can see that the pressure value at 10 ns is rapidly increased as compared with the value at 5 ns. This increase will be also due to the absorption of the laser beam energy by the plasma, as is seen in Fig 4(a). One can see from Fig. 4(c) that the plume velocity reaches the maximum value of about 20,000 m/s. At 10 ns, the velocity has a strong peak near the target. This excess kinetic energy is believed to be delivered by the absorption of the pulsed laser energy. In the calculated results for the case without plasma shielding effect, this feature was not seen, though the result is not presented here. The calculated profile of vapor density at each time is similar to the one for the vapor pressure given in Fig. 4(b). In the present calculation, because the vapor plume expands into vacuum, the contact surface between air and metallic vapor could not be recognized.

In Fig. 5, the temporal variation of the impulse value is compared between measurement and calculation. The calculated impulse data is given by integrating the computed pressure at the computational cell adjacent to the target surface. The time variation of the computed profile is plotted in Fig. 6. The time variation of the experimental pressure is deduced from the impulse data given in Fig. 5, and is presented also in Fig. 6. From Fig. 5, the measured and calculated impulse values are increased as time evolves. The calculated impulse profile reaches its plateau value of about 1.5. The present calculation replicates the measured impulse value after 20 ns. However, the calculation could not predict the onset of the impulse rise in the experiment; the calculated impulse generation is delayed in comparison to the measurement. In addition, the slope in the impulse profile given by calculation is steeper than the measured one.

This result can be explained by the pressure profile presented in Fig. 6. From the figure, one can see that the pressure begins to increase after 5 ns in the present calculation. The computed pressure is quickly increased up to about 200 MPa. After the pressure profile has its maximum value, the pressure is rapidly decreased. Contrary to the calculated result, the pressure starts increasing at least at 2 ns in the experiment after the target begins to be heated. In addition, the pressure is slowly decreased compared with the calculation, keeping the higher pressure compared with the calculated pressure.

It is found from the present computation that the measured impulse value can be obtained by selecting an appropriate value of the surface reflectivity, R_f. However, qualitative nature of the impulse generation characteristics was different between calculation and measurement. A possible cause for this difference may be due to neglecting other detailed physics such as Knudsen layer effect, or the penetration of the laser intensity into the target. Whether such more detailed modeling could explain the discrepancy seen in the present study remains to be investigated in the future.

IV. Concluding Remarks

A computational method is developed to calculate the laser ablation phenomena during pulsed laser heating. The method can be used to simulate the impulse generation during the laser-solid interaction. The calculated results indicate that the effect of the plasma shielding has a strong impact on the impulse generation for the case of the low background ambient pressure. In order to fully understand the impulse generation mechanisms by laser ablation, more detailed physical modeling is needed.

References

[1]Sasoh A., Mori K., Anju K., Shimono M., Sawada K., and Zaretsky E. "Laser-Ablative Propulsion Using Polyacetal at Low Ambient Pressures," AIAA Paper 2007-1185, January, 2007.

[2]Mori K., Anju K., Sasoh A., and Zaretsky E., "Impulse generation by ND:YAG laser ablation of aluminum," AIAA Paper 2007-1187, January, 2007.

[3]Bogaerts A., Chen Z., Renaat G., and Akos V. "Laser ablation for analytical sampling: what can we learn from modeling?," *Spectrochimica Acta*, Part B Vol.58, 2003, pp.1867-1893.

[4]Wada, Y., and Liou, M. S., "A Flux Splitting Scheme with High-Resolution and Robustness for Discontinuities," AIAA paper 94-0083, January, 1994.

[5]Spitzer, L., *Physics of Fully Ionized Gases*, Interscience Publishers, London, 1956, pp.147-149.

[6]Root, R. G., "Modeling of Post-Breakdown Phenomena," in *Laser-Induced-Plasmas and Applications*, Rakziemski, L. J., and Cremers, D. A. Eds, Marcel Dekker, Inc., New York, 1989, pp.69-103.

[7]Jeong S. H., Greif R., and Rosso R. E., "Numerical modeling of pulsed laser evaporation of aluminum targets," *Applied Surface Science*, Vol. 129, May 1998, pp.177-183.

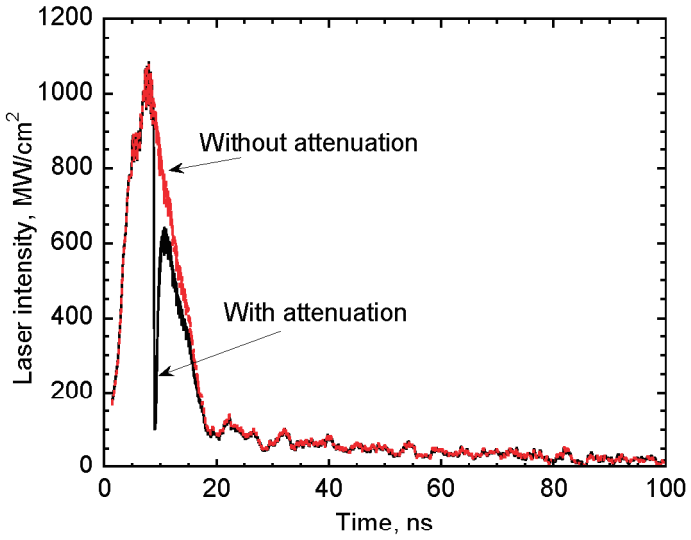

Figure 2. Comparison of time variation of incident laser intensity between with and without laser beam attenuation.

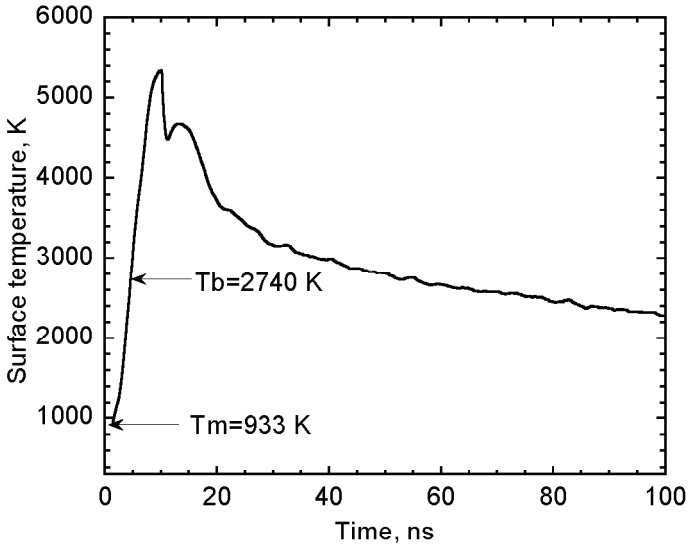

Figure 3. Time variation of calculated surface temperature

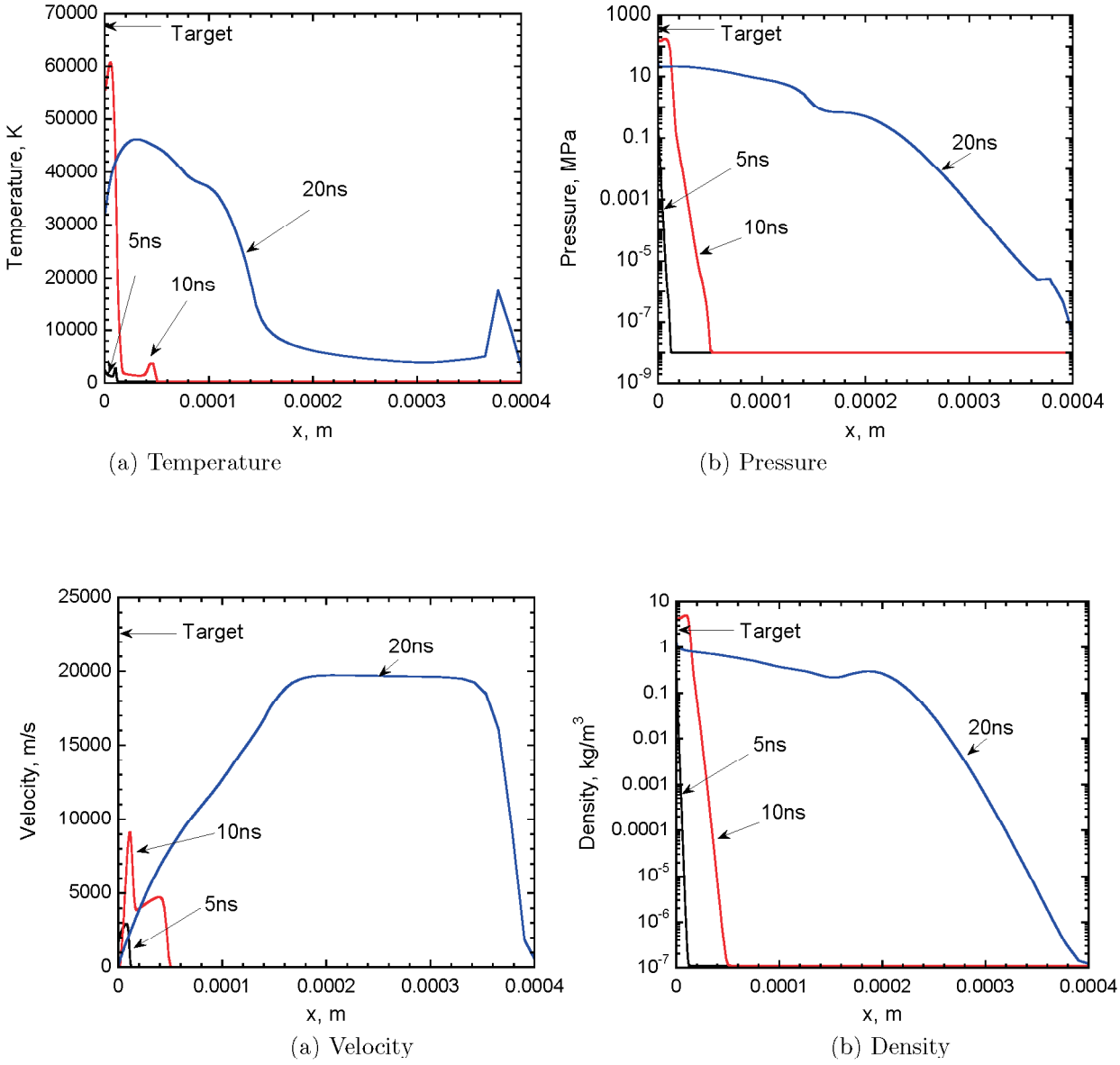

Figure 4. Calculated flow properties during pulsed laser heating

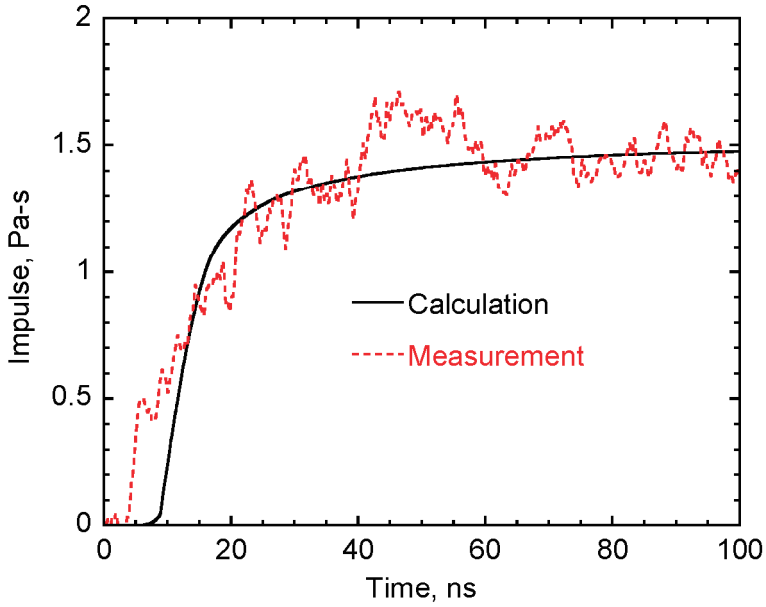

Figure 5. Comparison of impulse between measurement and calculation

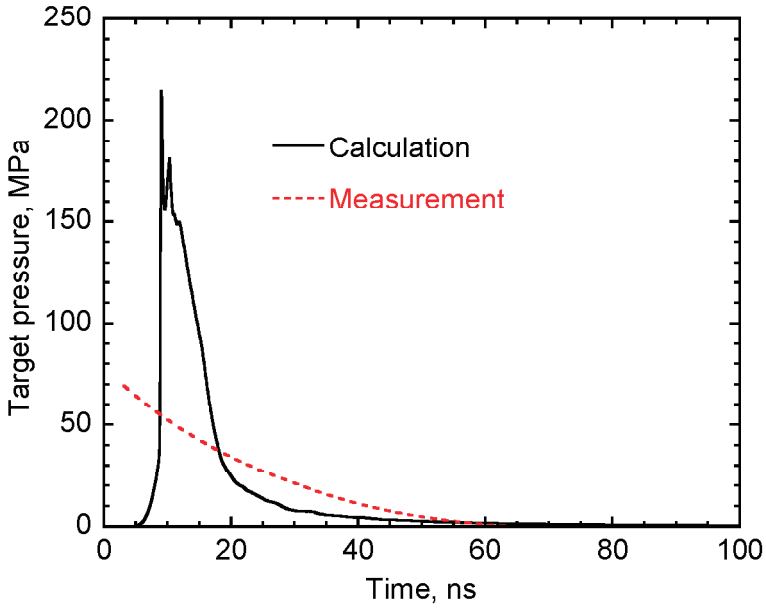

Figure 6. Comparison of target pressure between measurement and calculation